Supporting Information

Optical Control of Reactions between Water and Laser-Cooled Be^+ Ions

Tiangang Yang[1,], Anyang Li[2,*], Gary K. Chen[1], Changjian Xie[3], Arthur G. Suits[4], Wesley C. Campbell[1], Hua Guo[3] and Eric R. Hudson[1]*

[1]Department of Physics and Astronomy, University of California Los Angeles, Los Angeles, California 90095

[2]Key Laboratory of Synthetic and Natural Functional Molecule Chemistry, Ministry of Education, College of Chemistry and Materials Science, Northwest University, 710127 Xi'an, P. R. China

[3]Department of Chemistry and Chemical Biology, University of New Mexico, Albuquerque, New Mexico 87131

[4]Department of Chemistry, University of Missouri, Columbia, Missouri 65211

Corresponding Authors: yangtiangang@g.ucla.edu (Experiment), liay@nwu.edu.cn (Theory),

S1. Experiment

S1.1 Apparatus

The title reaction was performed in a radio-frequency linear quadrupole ion trap (LQT) and diagnosed with a time-of-flight (TOF) mass spectrometer as well as a Be^+ fluorescence imaging system, shown in Figure S1A. (A similar apparatus has been described in detail elsewhere,[1-3] and only a brief illustration is provided here to introduce the Be^+ ion laser-cooling and state control scheme.) The LQT radio-frequency trapping voltage was driven at $\Omega/2\pi = 3$ MHz with an amplitude of 200 V. The distance from the trap center to the electrodes is $r_0 = 6.85$ mm, and the trap is enclosed in a UHV chamber ($< 5 \times 10^{-10}$ Torr). The chamber is equipped with a leak valve for introducing neutral molecule reagents, whose partial pressures are measured by a residual gas analyzer (RGA) and an ion gauge. Be^+ ions were loaded into the trap via laser ablation of a beryllium metal target. A pulsed Nd/YAG laser (Continuum Minilite II, operating with ~2 mJ at 1064 nm and pulse width 10ns) was focused onto a metallic beryllium sample to load the ion trap with Be^+.[4] The trapped Be^+ ions were laser-cooled on the $^2P_{3/2} \leftarrow {}^2S_{1/2}$ (F =2) transition with a linearly-polarized 313 nm laser (TOPTICA PHOTONICS TA-FHG pro) detuned -20 MHz from resonance. To prevent optical pumping into the $^2S_{1/2}$ (F=1) state, a second laser beam, detuned by -1.250 GHz from the main cooling laser via two acousto-optic modulators (AOMs), was applied to repump population back into the Doppler cooling cycle. Both the main cooling and repumping laser were sent into another AOM providing two more beams that were further detuned by -200 MHz. These red detuned beams enable faster laser cooling of hot Be^+ ions at the beginning of loading.

A typical reaction study began with a Coulomb crystal of ≈100 Be^+ ions at time t = 0, as shown in Fig. S1B. In the absence of the deliberate introduction of a reagent gas, Be^+ ions

exhibit a trap lifetime of ≈ 450 s. This loss is induced by reactions with residual background gas in the chamber, which is primarily H_2.[4] Although the $Be^+ (^2P_{3/2}) + H_2 \rightarrow BeH^+ + H$ reaction is exothermic by 2.4 eV, the ion trap depth is ~ 6 eV for BeH^+ ions, and thus the charged product of this reaction is trapped. The trapped BeH^+ molecules created in to these 'background' reactions are visible as 'dark' ions in Figure S1C (apparent vacancies in the Coulomb crystal of fluorescing Be^+) and their presence was confirmed by the TOF mass spectrum shown in Figure S1B. In order to minimize the influence of background gas, all measurements were performed in ≈ 60 s. The influence of the background H_2 reaction in this timescale is negligible and considered as a loss rate in the rate measurement fitting, as shown in the TOF signal of Figure 1, there is no obvious BeH^+ peak emerging.

S1.2 Pressure Calibration

The manufacturer of the residual gas analyzer (RGA) used in this work does not provide an uncertainty for its absolute accuracy. We calibrate it by cross-correlating our RGA measurements with the total pressure measured by an Agilent UHV-24 Bayard-Alpert Gauge Tube. Although this ion gauge is quoted in the manual to have << 10% error at 5×10^{-10} Torr (our normal operation pressure), the fact that the ion gauge is set in a nipple connected to the chamber provides at least another 30% uncertainty. We calibrated the RGA to this ion gauge for H_2 and H_2O, finding mass dependent scaling factors for the RGA to ion gauge pressures of 0.58 for H_2, and 1.1 for H_2O. Using this calibrated pressure reading, our measured $Be^+ + H_2$ reaction rate coefficient of $(1.2 \pm 0.3_{stat}) \times 10^{-9}$ cm^3/s (Figure S3) agrees with existing literature[4] ($(1.3 \pm 0.4) \times 10^{-9}$ cm^3/s) within our estimated total uncertainty for the pressure measurement as described above.

S2. Theory

S2.1 Ground-state potential energy surface

The global potential energy surface (PES) for the $Be^+(^2S)$ + $H_2O(X^1A_1)$ → $BeOH^+(X^1\Sigma^+)$ + $H(^2S)$ reaction consists of a long-range (LR) term in the reactant asymptote and short-range (SR) term for the strongly interaction range. The former, which is important for an accurate description of the reaction kinetics, accounts for the leading electrostatic interactions between the two reactants when they are far apart. The latter, on the other hand, is obtained by fitting ab initio data. The two segments of the PES are connected smoothly via a switching function:

$$V = S_{global}V_{\mathrm{SR}} + \left(1 - S_{global}\right)V_{\mathrm{LR}}, \quad \text{(S1)}$$

$$S_{global} = \frac{1-\tanh[3(\xi-9.0)]}{2}, \quad \text{(S2)}$$

where ξ is the distance (in Å) between Be and O. the PES is dominated by V_{LR} for ξ > 9.5 Å, while by V_{SR} for ξ < 8.5 Å.

The LR PES can be written as:

$$V_{\mathrm{LR}} = V_{\mathrm{H_2O}} + V_{\mathrm{ES}}, \quad \text{(S3)}$$

where $V_{\mathrm{H_2O}}$ is the PES for the isolated H_2O molecule. This local PES is developed by a three-dimensional cubic spline interpolation of 792 ab initio points at the explicitly correlated unrestricted coupled cluster singles, doubles, and perturbative triples (UCCSD(T)) method[5] with a specially optimized triples zeta correlation consistent F12 basis set (VTZ-F12)[6] level, the same as the SR PES calculations (*vide infra*). All the potential energies of ab initio points are related to the potential minimum of H_2O at its equilibrium geometry. The electrostatic interactions V_{ES} between the Be^+ ion and H_2O molecule consists of several long-range terms. In describing these interactions, we assume that the water molecule is in its equilibrium geometry with the O atom in the *z* axis and the molecule is in the *yz* plane. *R* is the distance between Be^+ ion and the center of

mass of H_2O. We defined θ_x, θ_y and θ_z as the angles between the $\vec{R}$ vector and *x, y* and *z* axes, respectively. The leading electrostatic terms include the charge-dipole (proportional to R^{-2}), charge-quadruple (proportional to R^{-3}), and charge-induced dipole (proportional to R^{-4}) interactions:[7-8]

$$V_{\mathrm{ES}} = V_{\mathrm{c-d}} + V_{\mathrm{c-q}} + V_{\mathrm{c-id}}, \tag{S4}$$

where the charge-dipole interaction potential is:

$$V_{\mathrm{c-d}} = q\mu_{\mathrm{H_2O}} R^{-2} \cos\theta_z, \tag{S5}$$

the charge-quadruple interaction potential is:

$$V_{\mathrm{c-q}} = \frac{1}{2} qR^{-3}\left[\Theta_{zz}(3\cos^2\theta_z - 1) + \Theta_{xx}(3\cos^2\theta_x - 1) + \Theta_{yy}\left(3\cos^2\theta_y - 1\right)\right], \tag{S6}$$

and the charge-induced dipole interaction potential is:

$$V_{\mathrm{c-id}} = -\frac{1}{2} q\alpha R^{-4}\left[1 + \frac{\left|\alpha_{zz} - 1/2(\alpha_{xx}+\alpha_{yy})\right|}{3\alpha}(3\cos^2\theta_z - 1)\right]. \tag{S7}$$

For the H_2O molecule, the dipole moment $\mu_{\mathrm{H_2O}}$ is 1.855 Debye, the three non-zero quadruple moments Θ_{xx}, Θ_{yy} and Θ_{zz} are -2.5, 2.63 and -0.13 DÅ, and the polarizability α is 9.92 a.u. (α_{xx}, α_{yy} and α_{zz} are 10.31, 9.55 and 9.91 a.u.).[9]

For the SR PES, we first carried out ab initio calculations using the UCCSD(T)-F12a method[5] with a basis set VTZ-F12.[6] The stationary points along the reaction path are shown in Figure 3 and their geometries and energies are listed in Table S1. These ab initio points are then fit using the high-fidelity permutation invariant polynomial-neural network (PIP-NN) method.[10] In particular, 17 PIPs[11] up to second order have included as the input layer of the NN in order to take advantage of the permutation symmetry of this ABC_2 system. The NN consists of 2 layers, each with 20 and 60 interconnected neurons. The total number of parameters is thus 1681. The

details of the NN training can be found in ref. 10. The fitting is carried out in two different regions:

(a) The reactant asymptotic region V_1: There are 4457 points with the distance between Be and O from 4 Å to 50 Å. The RMSE of the fitting is only 0.01 kcal/mol (3 cm^{-1}).

(b) The main region V_2: There are 15834 points with the distance between Be and O less than 6 Å. The RMSE of the fitting is less than 0.4 kcal/mol (14 cm^{-1}).

The final SR PES V_{SR} is obtained by connecting these two fits with another switching function S_{fit}:

$$V_{fit} = S_{fit}V_1 + \left(1 - S_{fit}\right)V_2, \quad \text{(S8)}$$

$$S_{fit} = \frac{1-\tanh[3(\xi-5.0)]}{2}, \quad \text{(S9)}$$

As shown in Table S1, the PIP-NN PES faithfully reproduces energies and geometries of the stationary points. To assess the accuracy of the electrostatic potential (V_{ES}) in describing the long-range interactions, we have compared in Figure S4 its values to ab initio energies in the $Be^+ + H_2O$ asymptote in two orientations. The interaction is attractive when Be^+ approaches the O side along the C_2 axis of H_2O (a), while the interaction is repulsive as Be^+ approaches the H_2 side along the same axis (b). In both cases, the charge-dipole interaction dominates while other terms make small contributions. It is clear that the analytical potential provides a good representation of the ab initio values in the asymptotic region.

S2.2 Quasi-classical trajectory study of the $Be^+(^2S) + H_2O(X^1A_1)$ reaction

The quasi-classical trajectory (QCT) calculations were performed using VENUS.[12] The possible violation of the zero-point energy (ZPE) is a major deficiency in QCT method, particularly at low temperatures. This ZPE-violation problem is corrected using the approach

proposed by Paul and Hase.[13] Specifically, when a trajectory exits the strongly interacting region, the vibrational energy of $H_2O/BeOH^+$ in the reactant/product channel is calculated. If the energy is less than the ZPE, the momenta of all atoms in the system are reversed and the trajectory is forced back to the strongly interacting region without violating energy conservation. Only those trajectories with $H_2O/BeOH^+$ internal energies larger than the ZPEs are accepted.

The trajectories were initiated with a 41.0 Å separation between reactants, and terminated when products reached a separation of 8.0 Å. The atomic coordinates and momenta of the water reactant are sampled randomly using a Monte Carlo approach, based on a Boltzmann distribution at 300 K. The collision energy is sampled from a Boltzmann distribution of 100 K. The largest impact parameter was chosen b_{max}=39 Å to make sure the inclusion of long-range interactions. The propagation time step was chosen as 0.05 fs. The total energy conservation was found to be better than 0.029 kcal/mol for all the trajectories. A few trajectories were discarded if the propagation time reached 300 ps in each interval of two consecutive momentum reversing operations, or the number of momentum reversing exceeds 100.

The total reaction probability (P) for the title reaction is:

$$P = \frac{N_r}{N_{total}}, \tag{S10}$$

where N_r and N_{total} are the number of reactive trajectories and total number of trajectories, respectively. The capture probability is also computed analogously, except that a trajectory is counted as captured if the distance between Be^+ and O is less than 2.0 Å, and meanwhile this distance is shorter than any one of the two distances between Be^+ and H atoms. The thermal rate constant can be computed by the following expression:

$$k(T) = \left(\frac{8k_B T}{\pi\mu}\right)^{1/2} \pi b_{max}^2 P, \tag{S11}$$

where μ is the reduced mass between the two reactants, k_B the Boltzmann constant, and T temperature in Kelvin. In our calculations, a total of 29096 trajectories were run and the results are reported in the main text.

S2.3 Ab initio calculations of the $Be^+(^2P)$ + $H_2O(X^1A_1)$ reaction pathways

The electronically excited state PESs are much more complex than that of the ground electronic state because of the prevalence of electronic degeneracies. As a result, no global PESs have been developed for the reactions involving the excited state Be^+. Rather, ab initio calculations are carried out to map out the possible reaction pathways.

To understand the interaction in the reactant and product channels, the five lowest ^{2}A state potential energy curves along the $Be^{\cdots}OH_2$ coplanar (C_{2v}) geometry and along the $H^{\cdots}BeOH$ pseudo-linear ($\angle$O-Be-H =175^o) geometry are first determined at the complete active spaces self-consistent field (CASSCF)[14-15] level of theory with the full valence active space (9e,10o), using the augmented correlation-consistent valence triple zeta basis set (aug-cc-pVTZ).[16-17]The results are shown in Figure 4. Note that the equilibrium geometry of the excited $BeOH^+$ ion is bent, but a linear geometry was used in the CASSCF scan to be consistent with the ground state $BeOH^+$, which is linear. These cuts reveal the nonadiabatic pathways leading to the reactive as well as charge transfer channels, as discussed in the main text. The stationary points along the reaction path on the first excited state are optimized at the CASSCF/6-31G* level and corrected for dynamical correlations at the multi-reference configuration interaction (MRCI)[18-19] level with the aug-cc-pVTZ basis set. They are listed in Table S2.

References

(1) Schowalter, S. J.; Chen, K.; Rellergert, W. G.; Sullivan, S. T.; Hudson, E. R. An Integrated Ion Trap and Time-of-Flight Mass Spectrometer for Chemical and Photo-Reaction Dynamics Studies. *Rev. Sci. Instrum.* **2012,** *83*, 043103.

(2) Schneider, C.; Schowalter, S. J.; Chen, K.; Sullivan, S. T.; Hudson, E. R. Laser-Cooling-Assisted Mass Spectrometry. *Phys. Rev. Appl.* **2014,** *2*, 034013.

(3) Puri, P.; Mills, M.; Schneider, C.; Simbotin, I.; Montgomery, J. A.; Côté, R.; Suits, A. G.; Hudson, E. R. Synthesis of Mixed Hypermetallic Oxide $BaOCa^+$ from Laser-Cooled Reagents in an Atom-Ion Hybrid Trap. *Science.* **2017,** *357*, 1370-1375.

(4) Roth, B.; Blythe, P.; Wenz, H.; Daerr, H.; Schiller, S. Ion-Neutral Chemical Reactions between Ultracold Localized Ions and Neutral Molecules with Single-Particle Resolution. *Phys. Rev. A.* **2006,** *73*, 042712.

(5) Knizia, G.; Adler, T. B.; Werner, H.-J. Simplified CCSD(T)-F12 Methods: Theory and Benchmarks. *J. Chem. Phys.* **2009,** *130*, 054104.

(6) Peterson, K. A.; Adler, T. B.; Werner, H.-J. Systematically Convergent Basis Sets for Explicitly Correlated Wavefunctions: The Atoms H, He, B–Ne, and Al–Ar. *J. Chem. Phys.* **2008,** *128*, 084102.

(7) Stone, A. J. *The Theory of Intermolecular Forces*. Second Edition ed.; Oxford University Press: 2013.

(8) Buckingham, A. D. Permanent and Induced Molecular Moments and Long-Range Intermolecular Forces. *Adv. Chem. Phys.* **1967,** *12*, 107-142.

(9) NIST. Http://Cccbdb.Nist.Gov/Expdatax.Asp.

(10) Jiang, B.; Li, J.; Guo, H. Potential Energy Surfaces from High Fidelity Fitting of Ab Initio Points: The Permutation Invariant Polynomial-Neural Network Approach. *Int. Rev. Phys. Chem.* **2016,** *35*, 479-506.

(11) Braams, B. J.; Bowman, J. M. Permutationally Invariant Potential Energy Surfaces in High Dimensionality. *Int. Rev. Phys. Chem.* **2009,** *28*, 577–606.

(12) Hu, X.; Hase, W. L.; Pirraglia, T. Vectorization of the General Monte Carlo Classical Trajectory Program Venus. *J. Comput. Chem.* **1991,** *12*, 1014-1024

(13) Paul, A. K.; Hase, W. L. Zero-Point Energy Constraint for Unimolecular Dissociation Reactions. Giving Trajectories Multiple Chances to Dissociate Correctly. *J. Phys. Chem. A.* **2016,** *120*, 372-378.

(14) Knowles, P. J.; Werner, H.-J. An Efficient Second-Order MC SCF Method for Long Configuration Expansions. *Chem. Phys. Lett.* **1985,** *115*, 259-267.

(15) Werner, H. J.; Knowles, P. J. A Second Order Multiconfiguration SCF Procedure with Optimum Convergence. *J. Chem. Phys.* **1985,** *82*, 5053-5063.

(16) Dunning, T. H. Gaussian Basis Sets for Use in Correlated Molecular Calculations. I. The Atoms Boron through Neon and Hydrogen. *J. Chem. Phys.* **1989,** *90*, 1007-1023.

(17) Kendall, R. A.; Dunning, T. H.; Harrison, R. J. Electron Affinities of the First‐Row Atoms Revisited. Systematic Basis Sets and Wave Functions. *J. Chem. Phys.* **1992,** *96*, 6796-6806.

(18) Knowles, P. J.; Werner, H.-J. An Efficient Method for the Evaluation of Coupling Coefficients in Configuration Interaction Calculations. *Chem. Phys. Lett.* **1988,** *145*, 514-522.

(19) Werner, H. J.; Knowles, P. J. An Efficient Internally Contracted Multiconfiguration–Reference Configuration Interaction Method. *J. Chem. Phys.* **1988,** *89*, 5803-5814.

Table S1. Comparison of ab initio energies and geometries with those on the PIP-NN PES in internal coordinates of the stationary points for the $Be^+(^2S) + H_2O(X^1A_1) \rightarrow BeOH^+(X^1\Sigma^+) + H(^2S)$ reaction. (The hydrogen atoms in H_2O molecule are denoted as H1 and H2.)

Species	Method	E (eV)	r_{BeO} (Å)	r_{OH1} (Å)	r_{OH2} (Å)	θ_{H1OH2} (°)	θ_{BeOH1} (°)	$\phi_{BeOH1H2}$ (°)
$Be^+ + H_2O$	Ab initio	0.0		0.959	0.959	104.4		
	PES	0.0		0.959	0.959	104.4		
	Exp.	0.0		0.958	0.958	104.5		
$Be^{+\cdots}OH_2$	Ab initio	-2.74	1.561	0.971	0.971	109.6	125.2	180.0
	PES	-2.74	1.560	0.973	0.973	109.4	125.3	180.0
SP	Ab initio	-0.67	1.391	0.964	1.469	115.0	177.4	180.0
	PES	-0.68	1.393	0.965	1.454	115.3	178.3	180.0
$H^{\cdots}BeOH^+$	Ab initio	-0.99	1.329	0.952	3.100	0.0	180.0	180.0
	PES	-1.03	1.324	0.948	3.122	0.0	180.0	180.0
$BeOH^+ + H$	Ab initio	-0.32	1.323	0.953			180.0	180.0
	PES	-0.32	1.326	0.954				

Table S2. Energies (relative to $Be^+(^2S) + H_2O(X^1A_1)$) and geometries in internal coordinates of the stationary points for the $Be^+(^2P) + H_2O(X^1A_1) \rightarrow BeOH^+(a^3A'') + H(^2S)$ reaction on the first excited state. (The hydrogen atoms in H_2O molecule are denoted as H1 and H2.)

Species	E (eV)	r_{BeO} (Å)	r_{OH1} (Å)	r_{OH2} (Å)	θ_{H1OH2} (°)	θ_{BeOH1} (°)	$\phi_{BeOH1H2}$ (°)

$Be(^1S)+ H_2O^+(X^2B_1)$	3.55		1.013	1.013	108.0		
$Be^+(^2P)+ H_2O(X^1A_1)$	3.99		0.981	0.981	102.3		
IM1*	0.27	1.581	0.984	0.984	110.1	124.9	180.0
TS1*	1.10	1.636	1.046	1.105	95.2	109.4	76.4
IM2*	-0.30	1.619	0.991	2.946	180.0	180.0	180.0
$BeOH^+(a^3A'')+ H(^2S)$	3.85	1.701	0.999		126.7		

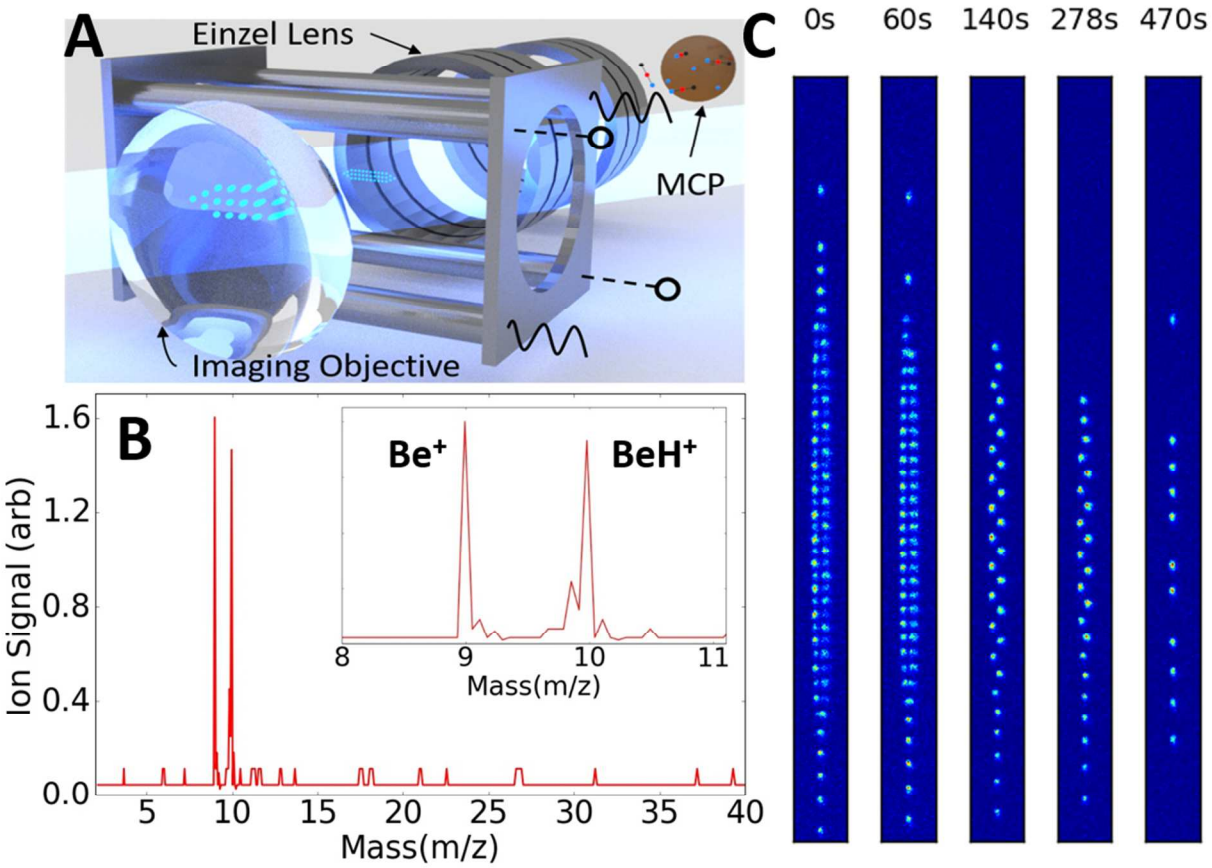

Figure S1. (A) A schematic of the experimental apparatus, including the LQT, the fluorescence imaging system, and the TOF. (B) A typical TOF trace after loading a hundred Be^+ ions for 300 s, indicating Be^+ ions reacting with residual H_2 gas is one reason for losing of Be^+ ions. (C) Be^+ ions fluorescence images at different reaction time. The lifetime of Be^+ ions in the trap is ≈450 s, the dark ions are BeH^+ from reaction $Be^+(^2P_{3/2}) + H_2 \rightarrow BeH^+ + H$.

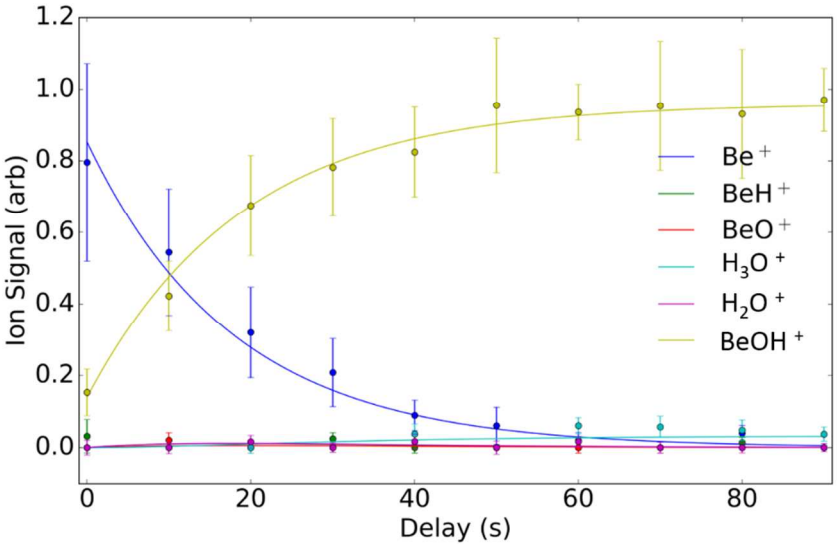

Figure S2. The temporal evolution of Be^+, BeH^+, BeO^+, H_3O^+, H_2O^+ and $BeOH^+$ in the trap as a function of reaction time as well as the solutions of differential equations fitted to the kinetics data with $P_P = 26\%$.

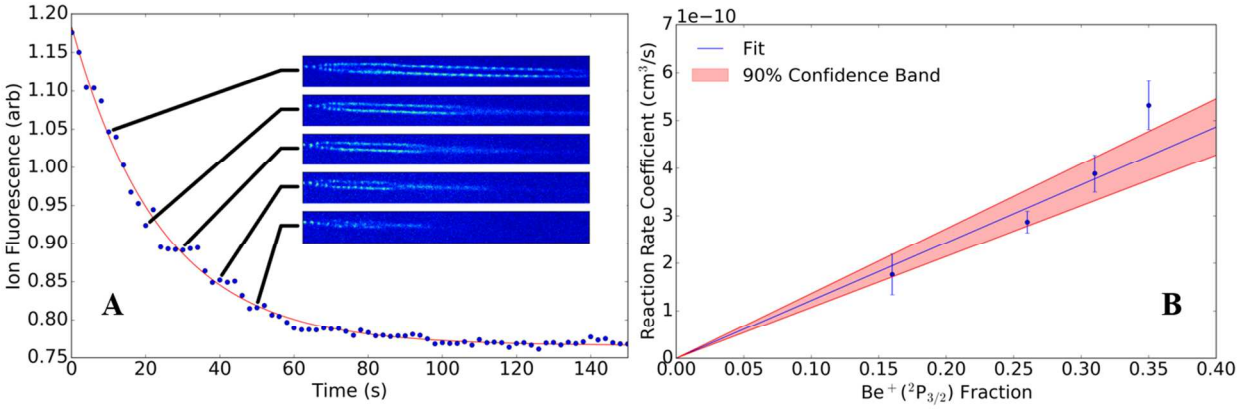

Figure S3. **(A)** A typical fluorescence decay measurement of $Be^+ + H_2$. The inset images are a subset of the original ion fluorescence images recorded by the camera. The red curve is an exponential fit (with a free offset) to the data, which gives the total reaction rate. **(B)** A fit of Be^+

+ H_2 fluorescence decay at various P state excitation fractions. A statistical rate coefficient for full excitation of $(1.2 \pm 0.3_{stat}) \times 10^{-9}$ cm^3/s is in agreement with existing literature.

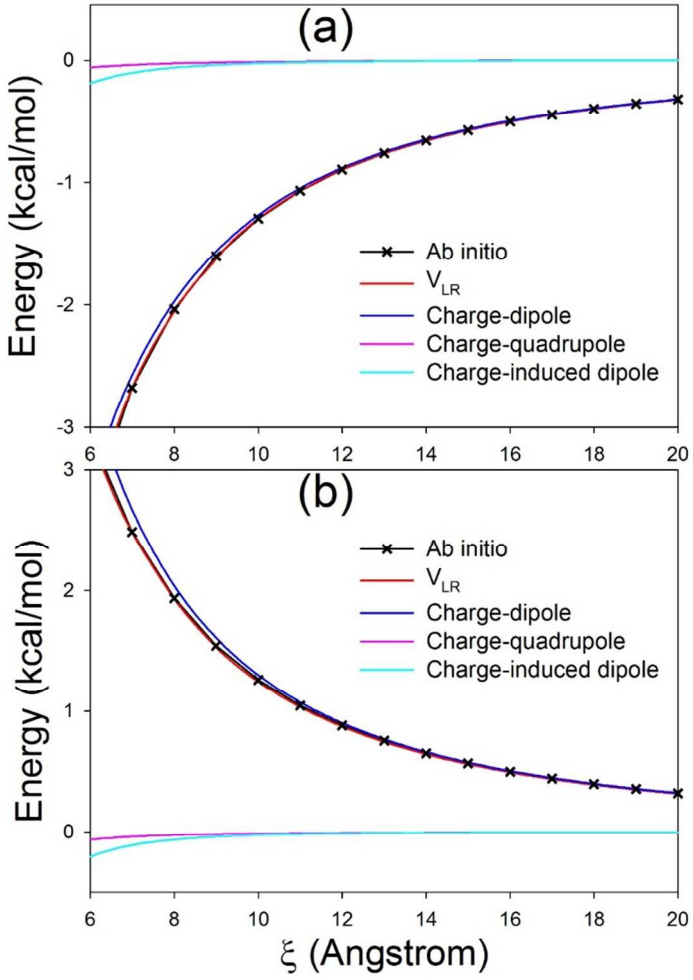

Figure S4: Comparison of the analytic long-range interaction potentials with the ab initio points in the $Be^+(^2S) + H_2O$ asymptote in two configurations: Be^+ approaching H_2O in the O (a) and H_2 ends (b) while maintaining the C_{2v} symmetry.